Inorg. Chem. **2003**, *42*, 4153–4159

New Ionic Crystals of Oppositely Charged Cluster Ions and Their Characterization

Jung Ho Son and Young-Uk Kwon*

Department of Chemistry and BK-21 School of Molecular Science, Sungkyunkwan University, Suwon 440-746, Korea

Oc Hee Han*

Solid-state Analysis Team, Daegu Branch, Korea Basic Science Institute and Department of Industrial Chemistry, Kyungpook National University, Daegu 702-701, Korea

Received January 15, 2003

By reacting Keggin-type polyoxometalate cluster anions $H_2W_{12}O_{40}^{6-}$ (metatungstate) or $Co^{II}W_{12}O_{40}^{6-}$ (tungstocobaltate) with the large aluminum cluster polycation $[Al_{30}O_8(OH)_{56}(H_2O)_{26}]^{18+}$, Keggin ion based molecular ionic compounds $[\delta\text{-}Al_{13}O_4(OH)_{24}(H_2O)_{12}][XW_{12}O_{40}](OH)\cdot nH_2O$ (X = H_2 (**1**) and Co (**2**); $n \cong 20$) and $[W_2Al_{28}O_{18}(OH)_{48}(H_2O)_{24}]$-$[H_2W_{12}O_{40}]_2\cdot 55H_2O$ (**3**) were obtained. The polygon-shaped cluster ions are packed alternately through intercluster hydrogen bonds as well as electrostatic interactions, leaving large pores, which result from the packing of large clusters. The clusters are arranged in square pyramidal geometries, showing face-to-face interactions between them. The isolation of metastable $[\delta\text{-}Al_{13}O_4(OH)_{24}(H_2O)_{12}]^{7+}$ and the formation of a new transition metal substituted aluminum heteropolycation $[W_2Al_{28}O_{18}(OH)_{48}(H_2O)_{24}]^{12+}$ in **1**–**3** result from the slow fragmentation and recombination of Al_{30} in the presence of suitable counter cluster anions with similar shape and charge.

Introduction

Building block approaches to design and construct new solid materials have become an important trend in synthetic inorganic chemistry.[1] Recently, clusters have been introduced in this field as building blocks. In most of the cases, the clusters form covalent bonds with metal cations or organic links to form extended networks.[2] There are a few compounds that are formed by ionic interactions between inorganic cluster ions and charged organic counterparts.[3] We have demonstrated that oppositely charged inorganic cluster ions can self-assemble to build three-dimensional architectures.[4,5] This class of solid can be considered as a cluster analogue of conventional ionic solids in that these solids are composed of oppositely charged ions of similar sizes and charges in both cases, and can be characterized by their large accessible pores because of the packing of large clusters of about 1 nm size.

The chemistry of Al^{3+} ion in aqueous systems remains challenging despite its long history. For example, two new aluminum polycations, $[\delta\text{-}Al_{13}O_4(OH)_{24}(H_2O)_{12}]^{7+}$ ($\delta\text{-}Al_{13}$) and $[Al_{30}O_8(OH)_{56}(H_2O)_{26}]^{18+}$ (Al_{30}), have been identified only recently.[6,7] While the latter was well characterized by X-ray single-crystal structure and ^{27}Al NMR spectroscopy, the former is known only for its crystal structure because it is reported to be an intermediate species and is obtained in a very small quantity.

As a continuation of our pursuit for constructing solid materials by combining charged cluster ions and to learn the

* Authors to whom correspondence should be addressed. E-mail: ywkwon@chem.skku.ac.kr (Y.-U.K); ohhan@kbsi.re.kr (O.H.H.).

(1) (a) Moulton, B.; Zaworotko, M. J. *Chem. Rev.* **2001**, *101*, 1629. (b) Cotton, F. A.; Lin, C.; Murillo, C. A. *Acc. Chem. Res.* **2001**, *34*, 759. (c) Müller, A.; Serain, C. *Acc. Chem. Res.* **2000**, *33*, 2. (d) Eddaoudi, M.; Moler, D. B.; Li, H.; Chen, B.; Reineke, T. M.; O'Keeffe, M.; Yaghi, O. M. *Acc. Chem. Res.* **2001**, *34*, 319. (e) Holliday, B. J.; Mirkin, C. A. *Angew. Chem., Int. Ed.* **2001**, *40*, 2022.

(2) (a) Finn, R. C.; Burkholder, E.; Zubieta, J. *Chem. Commun.* **2001**, 1852. (b) Kahn, M. I.; Yohannes, E.; Powell, D. *Inorg. Chem.* **1999**, *38*, 212. (c) Sadakane, M.; Dickman, M. H.; Pope, M. T. *Angew. Chem., Int. Ed.* **2000**, *39*, 2914.

(3) (a) Coronado, E.; Gómez-García, C. J. *Chem. Rev.* **1998**, *98*, 273. (b) Golhen, S.; Ouahab, L.; Grandjean, D.; Molinié, P. *Inorg. Chem.* **1998**, *37*, 1499.

(4) (a) Son, J. H.; Choi, H.; Kwon, Y.-U. *J. Am. Chem. Soc.* **2000**, *122*, 7432. (b) Son, J. H.; Kwon, Y.-U. *Bull. Kor. Chem. Soc.* **2001**, *22*, 1224.

(5) (a) Choi, H.; Kwon, Y.-U.; Han, O. H. *Chem. Mater.* **1999**, *11*, 1641. (b) Son, J. H.; Choi, H.; Kwon, Y.-U.; Han, O. H. *J. Non-Cryst. Solids* **2003**, *318*, 186.

(6) Allouche, L.; Gérardin, C.; Loiseau, T.; Férey, G.; Taulelle, F. *Angew. Chem., Int. Ed.* **2000**, *39*, 511.

(7) Rowsell, J.; Nazar, L. F. *J. Am. Chem. Soc.* **2000**, *122*, 3777.

10.1021/ic0340377 CCC: $25.00
Published on Web 06/04/2003

principles of structure building based on the cluster sizes, charges, and shapes, we have explored the system between Al_{30} and $[H_2W_{12}O_{40}]^{6-}$ (W_{12}, metatungstate) or $[Co^{II}W_{12}O_{40}]^{6-}$ (CoW_{12}, tungstocobaltate) polyoxometalate (POM) ions and obtained single crystals of $[\delta\text{-}Al_{13}O_4(OH)_{24}(H_2O)_{12}][XW_{12}O_{40}]\text{-}(OH)\cdot nH_2O$ ($X = H_2$ (**1**) and Co (**2**); $n \cong 20$) and $[W_2Al_{28}O_{18}\text{-}(OH)_{48}(H_2O)_{24}][H_2W_{12}O_{40}]_2\cdot 55H_2O$ (**3**). The crystal structures of **1**−**3** show the packing of the polygon-shaped cluster ions with their faces interacting through intercluster hydrogen bonds and electrostatic interactions. The formation of δ-Al_{13} in **1**, **2**, and a new heteropolycation $[W_2Al_{28}O_{18}(OH)_{48}\text{-}(H_2O)_{24}]^{12+}$ (W_2Al_{28}) in **3** implies that Al_{30} can be fragmented under suitable conditions to isolate metastable δ-Al_{13}, and the formed δ-Al_{13} can be subsequently reassembled to yield a new heteropolycation. In this paper, we describe the syntheses and crystal structures of **1**−**3,** and solid-state ^{27}Al NMR data of **1** and **2** to complete the characterization of δ-Al_{13}.

Experimental Section

Preparation of the Solutions. Solutions of Al_{30}, W_{12}, and CoW_{12} were prepared following the literature methods. A brief description on the synthesis procedure for each solution is given below.

Al_{30} Solution.[6,7] A 2 M NaOH solution was added dropwise into a 0.2 M $AlCl_3\cdot 6H_2O$ solution until the OH^-/Al^{3+} ratio became 2.3. The turbid solution was aged in an oven at 90 °C for 2 days to make a clear Al_{30} solution (pH 3.8).

W_{12} Solution.[8] A 6 M HCl solution was added into a 0.2 M $Na_2WO_4\cdot 2H_2O$ solution until the solution pH became 5. The solution was aged at room temperature for 1 week before use to ensure formation of W_{12}^{6-} ions. The solution pH was about 5.7 after aging.

CoW_{12} Solution.[9] $Na_2WO_4\cdot 2H_2O$ (9.9 g) was dissolved in 20 mL water, and 1.5 mL of glacial acetic acid was added. While the solution was being heated, a 6 mL aqueous solution containing one drop of glacial acetic acid and 1.25 g of dissolved cobaltous acetate was added. The solution mixture was boiled for 15 min; thereafter, 7 g of KCl was added, and the mixture was cooled. The solids formed were filtered and added into 20 mL of 2 M H_2SO_4 solution. Undissolved solid was removed by filtration. The pH of the filtrate solution of CoW_{12} was below 1. Because aluminum polycationic species to be reacted with are unstable with respect to the decomposition into monomers at low pH, the solution pH was adjusted to about 4 by adding a 2 M NaOH solution before further reactions.

Single-Crystal Syntheses. Crystals of the title compounds **1** and **2** were obtained from the reactions between Al_{30} and W_{12} solutions and Al_{30} and CoW_{12} solutions, respectively. Because simply mixing the polycation and polyanion solutions gives rise to fast precipitate reaction without crystal formation, we have devised a simple apparatus to induce slow diffusion reactions between the reacting solutions similarly to the previously reported diffusion methods using membranes.[10] The cation and anion solutions were separately placed in 50 mL glass ampules ($\Phi = 25$ mm, $l = 100$ mm). The volumes of the solutions were adjusted to make the Al/W ratio 13/12. Distilled water was added to fill up the ampules, and the ampules were tightly covered with membranes of 0.2 μm pores. The two ampules were connected through a glass tube ($\Phi = 25$ mm, $l = 20$ mm), which was filled up with water. The assembly of the ampules and the tube, now 220 mm long and composed of three partitions along the length, was laid horizontally to start mutual diffusion reactions through the membranes into the central water pool. Initially, there formed powdery precipitates. After a few days, elongated colorless crystals of **1** or greenish-blue crystals of **2** grew out of the precipitates from the respective reactions. The single crystals were isolated from the precipitates by careful decantation of the solutions. The yields of the crystals were 3.1% for **1** and 1.5% for **2** based on Al. While storing crystals of **1** in its mother liquor for a few months without precipitates, small amount of block-shaped colorless crystals of **3** grew among the crystals **1**. Because of the distinct crystal shapes, the two crystals were easily discernible under a microscope and separated mechanically. Elemental anal. (wt %). Calcd for **1**: Al, 8.21; W, 51.63. Found: Al, 8.24; W, 51.41. Calcd for **2**: Al, 8.15; W, 51.26; Co, 1.37. Found: Al, 8.21; W, 50.96; Co, 1.27. Calcd for **3**: Al, 9.05; W, 57.23. Found: Al, 8.58; W, 58.08.

X-ray Single-Crystal Structure Determinations. The crystals were placed in glass capillary tubes with respective mother liquors, and the tubes were sealed with wax. Without the mother liquors the crystals decay quickly within a few hours. Crystal and intensity data were collected at 293(2) K using a Siemens 1K CCD diffractometer with graphite-monochromated Mo Kα radiation (0.71073 Å). A hemisphere of reflection data was collected as ω scan frames with a width of 0.3°/frame and exposure time of 20 s/frame. Cell parameters were determined and refined by the SMART program.[11] Data reduction was performed using SAINT software, which corrects for Lorentz and polarization effects.[12] Empirical absorption correction was applied with the SADABS program.[13] The positional parameters of the metal atoms and most of the cluster oxygen atoms were determined by the direct method (SHELXS-97).[14] Several cycles of refinement and difference Fourier synthesis (SHELXL-97) revealed the other atoms including the lattice water molecules.[15] The oxygen atoms of the lattice water molecules were refined with partial occupancies. For the structures of **1** and **2**, one of the lattice water oxygen atoms should be that of OH^- to meet the charge-balancing condition, but could not be located because of the disordered nature of the water molecules. Hydrogen atoms could not be found in the crystal structure refinements because of their low electron densities. All of the atoms were refined with anisotropic temperature factors. Detailed crystallographic parameters and averaged metal−oxygen bond distances of the cluster ions in the crystals are given in Tables 1−3.

Characterization. Thermogravimetric (TG) analyses were carried out by using the simultaneous TGA−DTA analysis module of a TA4000/SDT2960 thermogravimetric analyzer with a heating rate of 5 °C/min up to 1200 °C in an air flow. The TG curves of **1** (**2**) showed weight loss of 8.81% (8.29%) until 140 °C, corresponding to 21 (20) H_2O per formula unit, in agreement with the crystallographic data (22 and 19 H_2O for **1** and **2**, respectively). Water losses from the ligand water and hydroxyl groups follow by about 10.37% (9.86%) in the region of 140−800 °C, after which no weight changes were observed. The products after calcining the crystals above 800 °C showed powder XRD peaks of Al_2O_3 and

(8) Griffith, W. P.; Lesniak, P. J. B. *J. Chem. Soc. A* **1969**, 1066.
(9) Walmsley, F. *J. Chem. Educ.* **1992**, *69*, 936.
(10) (a) Hulliger, J. *Angew. Chem., Int. Ed. Engl.* **1994**, *33*, 143. (b) Madjid, A. H.; Vaala, A. R.; Pedulla, J.; Anderson, W. F. *Phys. Status Solidi A* **1972**, *12*, 575.
(11) *SMART*, version 5.0; data collection software; Bruker AXS, Inc.: Madison, WI, 1998.
(12) *SAINT*, version 5.0; data integration software; Bruker AXS, Inc.: Madison, WI, 1998.
(13) Sheldrick, G. M. *SADABS, A program for absorption correction with the Bruker SMART system*; Universitat Göttingen: Göttingen, Germany, 1996.
(14) Sheldrick, G. M. *SHELXS-97*; University of Göttingen: Göttingen, Germany, 1997.
(15) Sheldrick, G. M. *SHELXL-97*; University of Göttingen: Göttingen, Germany, 1997.

Table 1. Crystallographic Data for **1**−**3**

	1	**2**	**3**
chemical formula	$Al_{13}O_{103.08}W_{12}$	$Al_{13}CoO_{99.99}W_{12}$	$Al_{14}O_{112.83}W_{13}$
fw	4206.30	4215.79	4573.01
space group	*Pnma* (No. 62)	*Pnma* (No. 62)	$P2_1/c$ (No. 14)
a (Å)	28.107(5)	28.0614(14)	15.9154(13)
b (Å)	13.878(2)	13.9292(7)	16.2032(12)
c (Å)	25.137(4)	25.3690(12)	44.491(4)
β (deg)			98.019(2)
V (Å^3)	9805(3)	9916.1(8)	11361.1(16)
Z	4	4	4
D_{calcd} (g cm^{-3})	2.849	2.824	2.674
μ (mm^{-1})	14.259	14.257	13.332
R1[a]/wR2[b] (F_o, $I > 2\sigma$)	0.0596/0.1357	0.0388/0.1088	0.0541/0.1245
R1[a]/wR2[b] (F_o, all data)	0.0983/0.1569	0.0630/0.1194	0.1221/0.1448

[a] $R1 = \sum||F_o| - |F_c||/\sum|F_o|$. [b] $wR2 = \{\sum[w(F_o^2 - F_c^2)^2]/\sum[w(F_o^2)^2]\}^{1/2}$, $w = 1/[\sigma^2(F_o^2) + (aP)^2 + bP]$, where $P = [2F_c^2 + \mathrm{Max}(F_o^2,0)]/3$.

Table 2. Average Bond Lengths for $[\delta\text{-}Al_{13}O_4(OH)_{24}(H_2O)_{12}]^{7+}$ in **1** and **2**, and $[W_2Al_{28}O_{18}(OH)_{48}(H_2O)_{24}]^{12+}$ in **3**

	1	**2**	**3**
Al−O_{Td}[a]	1.834(11)	1.824(8)	1.846(9)
Al−O_{Td}	1.798	1.800	1.788
Al−O_{Oh}	1.994	1.991	2.005
Al−OH	1.878	1.875	1.875
Al−OH_2	1.926	1.927	1.918
W=O_{term}			1.721(10)
W−$O_{\mu 2}$			1.816
W−$O_{\mu 3}$			2.064
W−OH			2.254(9)

[a] Toward the rotated Al_3O_{13} triad.

Table 3. Average Bond Lengths for $[XW_{12}O_{40}]^{6-}$ (X = H_2 for **1** and **3**, and Co for **2**)

	1	**2**	**3**
W=O_{term}	1.716	1.711	1.717
W−O_{cor}	1.909	1.915	1.905
W−O_{edg}	1.940	1.948	1.935
W−$O_{\mu 3}$	2.208	2.163	2.207
Co−$O_{\mu 3}$		1.890	

WO_3. The TG curve of **3** was similar to those of **1** and **2** with weight loss of 7.22% until 140 °C, corresponding to 38 H_2O per formula unit, smaller than that found in the crystallographic data of **3** (55H_2O). It is probably because the crystal **3** is very efflorescent, easily loosing water.

IR spectra were obtained with a Nicolet 1700 FT-IR spectrometer using KBr disks dispersed with sample powders in the 4000−400 cm^{-1} range. Representative bands: **1**, 1067 (w, Al−OH_{bend}),[16] 932 (m, W=O), 889 (m, W−O_{edg}−W),[17] 770 (s, W−O_{cor}−W,Al−O_{Td}),[18] 648 (m, Al−OH_{Oh}), 555 (m, Al−O_{Oh});[19] **2**, 1075 (w), 945(m), 881 (m), 757 (s), 621 (m), 557 (m); **3**, 1091 (w), 932 (m), 884 (m), 768 (s), 541 (vs).

^{27}Al solid-state magic angle spinning (MAS) NMR spectra were obtained with a Bruker DSX 400 spectrometer. The sample spinning rate, the pulse length, and the pulse repetition delay employed were 13 kHz, 8 μs, and 1 s, respectively, when the solution 90° pulse length was 5 μs.

Magnetic properties of the crystal **2** were measured with the Quantum Design SQUID MPMS-5S magnetometer in the temperature range 2−300 K under a magnetic field of 10K gauss in order to confirm the divalent nature of Co in CoW_{12}. The magnetic susceptibility vs temperature plot shows a typical Curie behavior in the temperature range 2−300 K. The effective magnetic moment calculated from these data is 4.37 μ_B and compares well with the literature data on potassium tungstocobaltate ($K_5H[Co^{II}W_{12}O_{40}]$) of 4.27 μ_B.[20]

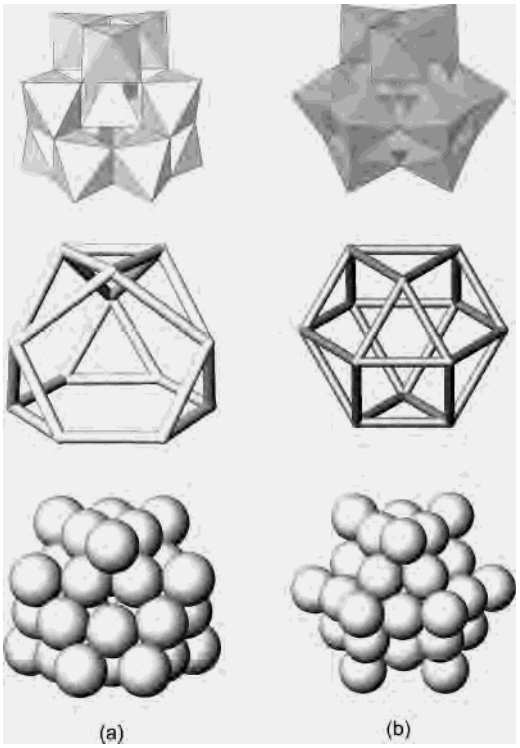

Figure 1. Polyhedral representations, approximated shapes, and space-filling models of (a) δ-Al_{13} and (b) W_{12} in **1**−**3**.

Results and Discussion

Structures of Cluster Ions in 1−3. All the cluster ions in **1**−**3** have either α- or δ-Keggin structures, or a dimeric structure of δ-Keggin ion (W_2Al_{28}). Keggin structures are based on four M_3O_{13} triads, which are edge- or corner-sharing to each other.[21] The structure of well-known ϵ-Al_{13} can be approximated as an ideal truncated tetrahedron, with four edge-sharing Al_3O_{13} triads forming four wide hexagon-shaped faces between them. The δ-Al_{13} polycation in **1** and **2** has the δ-Keggin structure, with one of the four edge-sharing Al_3O_{13} triads of the ϵ-Al_{13} rotated by 60° along its C_3 axis. While the ϵ-Al_{13} is highly symmetric (T_d), δ-Al_{13} has a lower symmetry (C_{3v}) due to the rotated Al_3O_{13} triads. The shape of δ-Al_{13} can be approximated as a modified truncated tetrahedron, with one hexagon-shaped face and three pentagon-shaped faces alongside of the rotated Al_3O_{13} triad (Figure 1a). The W_{12} and CoW_{12} polyanions in **1**−**3** have the α-Keggin structure with four W_3O_{13} triads connected to the others through corner sharing. The tetrahedral center of the polyanion is occupies by two protons in W_{12} or a Co^{II} in CoW_{12}. The shape of W_{12} can be approximated as a cuboctahedron with an O_h symmetry

(16) (a) Nakamoto, K. *Infrared Spectra of Inorganic and Coordination Compounds*; John Wiley & Sons: New York, 1963; p 159. (b) Glemser, O. *Nature* **1959**, *183*, 1476.
(17) Fournier, M.; Thouvenot, R.; Rocchiccioli-Deltcheff, C. *J. Chem. Soc., Faraday Trans.* **1991**, *87*, 349.
(18) Nomiya, K.; Kobayashi, R.; Miwa, M. *Bull. Chem. Soc. Jpn.* **1983**, *56*, 2272.
(19) Bradley, S. M.; Kydd, R. A.; Fyfe, C. A. *Inorg. Chem.* **1992**, *31*, 1181.
(20) Simmons, V. E. Doctoral Dissertation, Boston University, 1963.
(21) (a) Baker, L. C. W.; Figgis, J. S. *J. Am. Chem. Soc.* **1970**, *92*, 3794. (b) Keggin, J. F. *Nature* **1933**, *131*, 908.

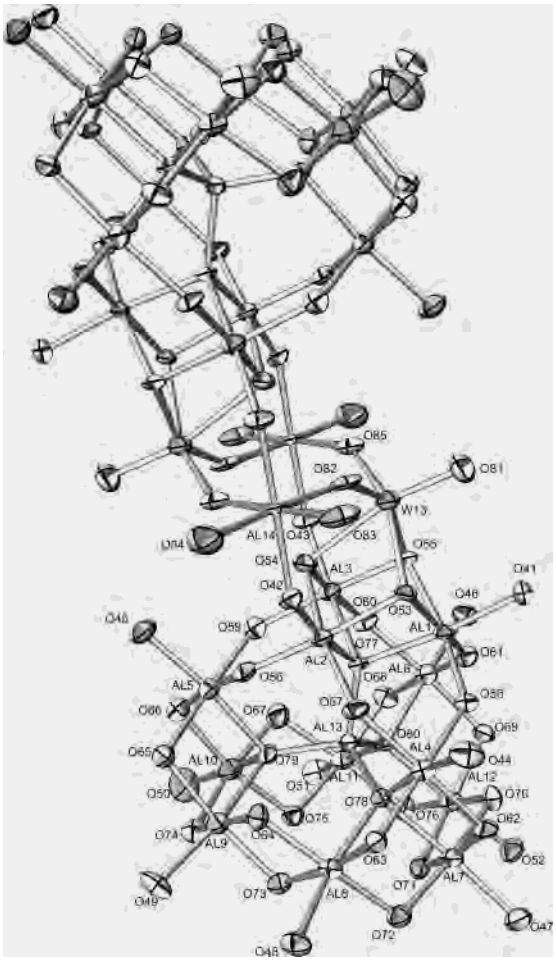

Figure 2. Thermal ellipsoid drawing of W_2Al_{28} cluster in **3** with atomic labels. Upper part of W_2Al_{28} in the figure is related to the lower part by an inversion symmetry.

(Figure 1b). The structural details of δ-Al_{13}, W_{12}, and CoW_{12} in **1**−**3** agree well with those found in the literature.[7,22,23]

The structure of the W_2Al_{28} cluster in **3** is analogous to that of Al_{30}, with the two capping AlO_6 octahedra of the two δ-Al_{13} units in Al_{30} replaced by two WO_6 (Figure 2). There is some evidence that supports the assignment of the capping WO_6. The structure refinement and difference Fourier synthesis show that there are considerably larger electron densities at these sites than the other Al sites, suggesting much heavier elements than Al. The charge balance consideration also excludes the possibility for the Al_{30}^{18+} cluster, which would require three W_{12}^{6-} clusters as opposed to the present 1:2 ratio. In addition, while the capping Al in Al_{30} have Al−O bond lengths (1.833(7)−1.965(6) Å) similar to those of peripheral aluminum octahedra of the δ-Al_{13} units,[6,7] the corresponding bond lengths at the capping sites in **3** show a wider range (1.721(10)−2.255(9) Å), comparable to the W−O distances of W_{12} in **3** (1.682(13)−2.276(11) Å), indicating heavily distorted octahedra, which is a prominent characteristic feature of a WO_6 octahedron.[24] In the Al_{30} structure, there are one terminal

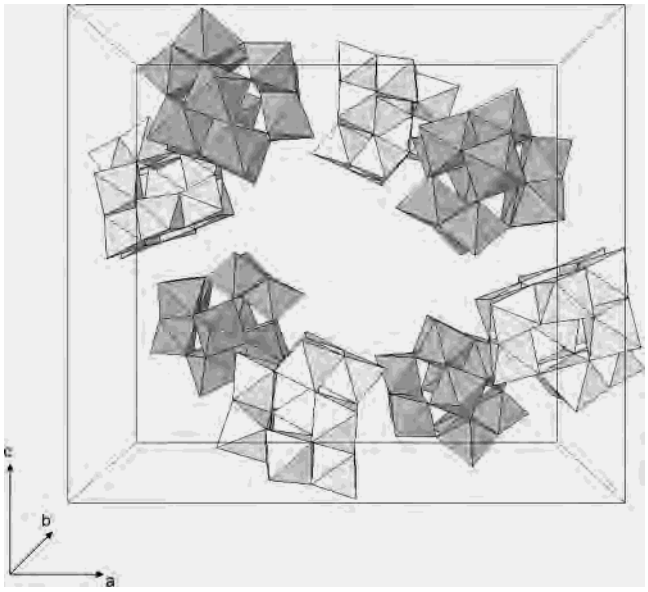

Figure 3. Unit cell content of **1** with four pairs of δ-Al_{13} (bright) and W_{12} (dark) clusters seen along the [010] direction.

H_2O and five bridging OH groups in each of the capping AlO_6 octahedron. Apparently, the substitution of Al^{3+} by W^{6+} is accompanied by deprotonation of these H_2O and OH groups. The terminal O81 has a short W−O distance (1.721(10) Å), indicative of a W═O bond. While the four W−O bonds cis to the W═O bond have intermediate bond distances (1.814(9)−2.106(8) Å), O54 which is trans to the W═O bond has a long W−O distance (2.255(9) Å), indicating an OH group. Therefore, the capping WO_6 has five O^{2-} ligands (one terminal, two μ_2, and two μ_3-bridging) and a μ_3-OH ligand, and the formula of the cluster can be written as $[W_2Al_{28}O_{18}(OH)_{48}(H_2O)_{24}]^{12+}$. W_2Al_{28} is the first example of the transition metal substituted aluminum polycation species.

Crystal Structures. The crystal structures of **1** and **2** are identical except for the difference between W_{12} and CoW_{12}. There are four symmetry-related δ-Al_{13} and W_{12} cluster pairs in each unit cell in the structure of **1** (Figure 3). The oppositely charged cluster pairs are arranged alternately to form distorted eight-membered rings with 1-D pores running along the *b*-direction (Figure 4). The pore dimension is calculated to be 12.8 × 7.4 Å^2 using the crystal data and subtracting the van der Waals radii of oxygen atoms. Water molecules and charge balancing OH^- ions fill the void volume between the cluster ions, which is calculated to be 43.8% of the total volume by using ionic radii of the atoms in the clusters.[25]

The crystal structure of **3** can be described with layers of W_2Al_{28} clusters parallel to the *bc*-plane of the unit cell and W_{12} clusters located between the W_2Al_{28} layers forming sandwich layers of $W_{12}-W_2Al_{28}-W_{12}$, that are stacked along the *a*-direction (Figure 5). The crystal structure shows 3-D interconnected pores running in the [100], [010], and [101] directions with the pore dimensions of 6.3 × 3.4, 7.0 × 3.4, and 4.8 × 5.1 Å^2, respectively, whose volumes sum up to 48.2% of the total volume.

(22) Seguin, L.; Gerand, B.; Nowogrocki, G. *Eur. J. Solid State Inorg. Chem.* **1995**, *32*, 181.
(23) Casañ-Pastor, N.; Gomez-Romero, P.; Jameson, G. B.; Baker, L. C. W. *J. Am. Chem. Soc.* **1991**, *113*, 5658.
(24) Kunz, M.; Brown, I. D. *J. Solid State Chem.* **1995**, *115*, 395.
(25) Spek, A. L. *PLATON, A Multipurpose Crystallographic Tool*; Utrecht University: Utrecht, The Netherlands, 2001.

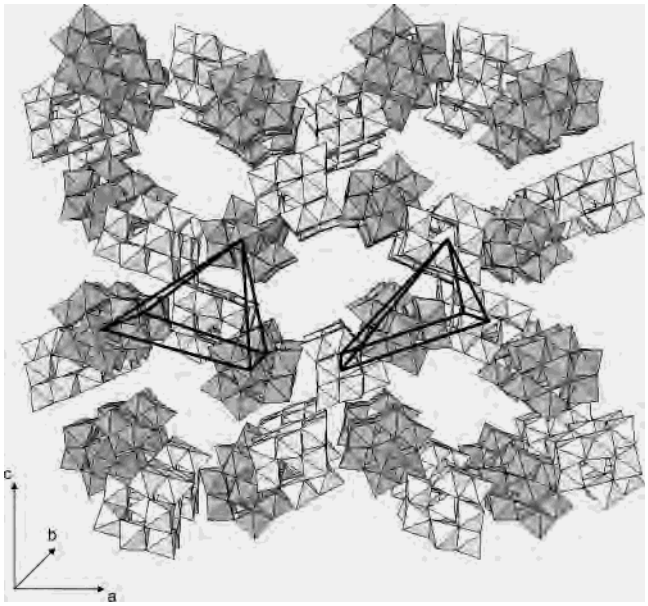

Figure 4. Extended view of the crystal structure of **1** along the [010] direction. Square pyramidal arrangements of the cluster ions around a δ-Al_{13} (left) and a W_{12} (right) are marked with bold lines.

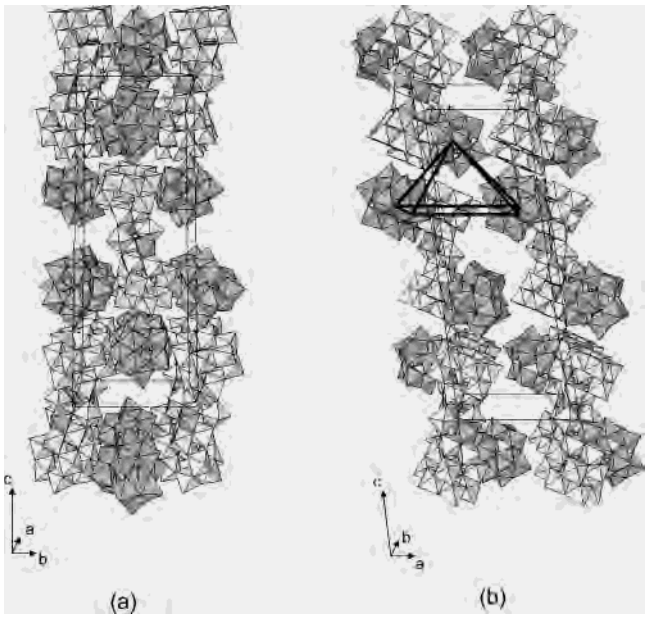

Figure 5. Crystal structure of **3** (W_2Al_{28}, bright; W_{12}, dark) viewed along the (a) [100] and (b) [010] directions. The square pyramidal arrangement of W_{12} around a δ-Al_{13} unit is marked with bold lines.

Details of the crystal structure provide some insights into the nature of the interactions between the cluster ions. In the structure of **1**, each δ-Al_{13} cluster has five neighboring W_{12} clusters in a square pyramidal geometry (Figures 4 and 6). The apical W_{12} has its square face almost parallel to the wide hexagon-shaped face of δ-Al_{13} allowing six hydrogen bonds between them. Among the four W_{12} in the basal plane of the square pyramid, two W_{12} have their triangular faces directed toward the two pentagonal faces of δ-Al_{13} and form four hydrogen bonds each. Another two W_{12} have their edges hydrogen bonded with two edges of a pentagonal face of δ-Al_{13}. Similarly, each W_{12} cluster has five neighboring

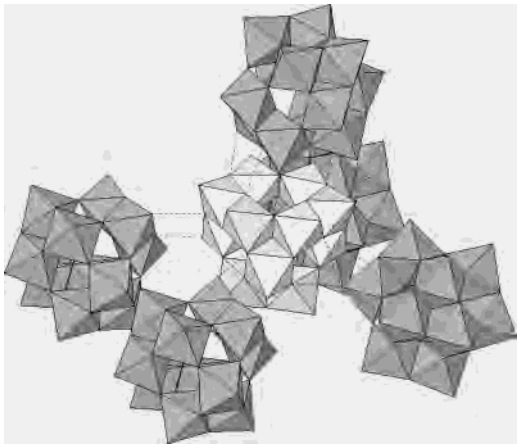

Figure 6. Square pyramidal arrangement of W_{12} around δ-Al_{13} with hydrogen bonds (dotted lines) in **1**.

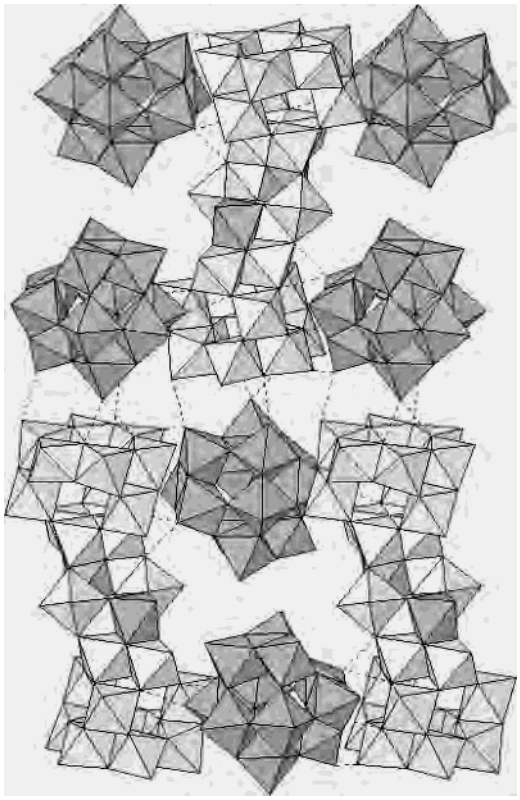

Figure 7. Arrangement of W_2Al_{28} and W_{12} in the sandwich layer of $W_{12}-W_2Al_{28}-W_{12}$ with hydrogen bonds (dotted lines) in the crystal structure of **3**.

δ-Al_{13} clusters in a distorted square pyramidal geometry. In the structure of **3**, as in the structure of **1**, five W_{12} clusters in a square pyramidal arrangement surround each δ-Al_{13} unit of W_2Al_{28}. However, the relative dispositions of the clusters in **3** are different from those in **1** (Figure 7). For example, the wide hexagon-shaped face of the δ-Al_{13} unit is in contact with a small triangular face of W_{12} with four hydrogen bonds. While two W_{12} clusters in the same $W_{12}-W_2Al_{28}-W_{12}$ layer are hydrogen bonded with pentagonal faces of two δ-Al_{13} units through their triangular faces similarly in the structure of **1**, another two W_{12} clusters in the next layer are relatively far apart with one weak hydrogen bond (3.27 Å), rendering

weak interaction between the $W_{12}-W_2Al_{28}-W_{12}$ layers (Figure 5b).

A way to view the packing of the cluster ions in the crystal structures of **1**−**3** is an analogy to the packing of ions in conventional compounds such as NaCl. In the latter cases, the arrangements of ions are highly symmetric with probably the highest packing densities and Madelung energies. Deviations from the highly symmetric structures are found when additional factors, such as bond covalency and inert pair effects, are involved.[26] These effects are paralleled with the intercluster hydrogen bonds and the low symmetric shapes of the clusters, respectively, in the present system.

The packing of building blocks of 1−2 nm size leaves accessible pores that are occupied by water and OH^-. In our previous study, $[\epsilon\text{-}AlO_4Al_{12}(OH)_{24}(H_2O)_{12}][Al(OH)_6Mo_6O_{18}]_2\text{-}(OH)\cdot 29.5H_2O$ crystals showed reversible water desorption−adsorption properties accompanied with destruction and reconstruction of the crystal structure.[4a] However, compounds **1**−**3** do not recover their respective structures when placed in humid atmosphere after removal of lattice water molecules by heating to 120 °C.

Formation of δ-Al_{13} and W_2Al_{28} Clusters. It is generally accepted that δ-Al_{13} occurs as an intermediate during the conversion of ϵ-Al_{13} into Al_{30} under forced hydrolysis conditions at high temperatures (>80 °C) as in the sequence ϵ-$Al_{13} \rightarrow \delta$-$Al_{13} \rightarrow Al_{30}$, and that it is unstable, precluding quantity sampling.[6,7] On the contrary, the compounds in this paper were obtained by decomposing the more stable Al_{30}. The major difference between our experiments and those in the literature lies in that we have used large W_{12} or CoW_{12} as counteranions and lower temperature. It is likely that the immediate precipitates formed upon diffusing Al_{30} and W_{12} solutions in our experiments have Al_{30} as the major Al species. The fact that the crystals of **1** and **2** are grown from these precipitates suggests that the strongly Al_{30} favoring equilibrium between δ-Al_{13} and Al_{30} can be reverted by having counteranions of suitable sizes and charges. Probably, the room temperature condition for the crystal growth in our study also aided the stabilization of δ-Al_{13} and kinetically prevented it from converting back to ϵ-Al_{13}.

In addition, since the δ-Al_{13} cluster itself is metastable, it would readily undergo a dimerization reaction if bridging metal ions were provided. If there were no other metal but aluminum, it would convert back into Al_{30}. However, during the storage of **1** in the mother liquor for a long time, parts of the δ-Al_{13} and W_{12} clusters would have slowly dissolved into the solution and W_2Al_{28} would have formed by dimerization of δ-Al_{13} in the presence of a small amount of tungstate ions or fragments of W_{12} clusters in the mother liquor, subsequently forming compound **3**. Because the formation of **3** was very slow (a few months) and the yield was low, we tried various reactions to synthesize W_2Al_{28} or crystal **3**, with no success: (1) An attempted hydrolysis of a solution containing Na_2WO_4:$AlCl_3$ = 1:14 similarly to the synthesis method of Al_{30} failed because of the precipitate formation between WO_4^{2-} and Al^{3+}. (2) Slow addition of a stoichiometric amount of Na_2WO_4 solution into ϵ-Al_{13} solution and further heating for 4−5 h at 127 °C gave a slightly turbid solution, and a reaction with W_{12} yielded crystals of **1**. (3) Synthesis of Al_{30} solution followed by slow addition of a stoichiometric amount of Na_2WO_4 solution and further heating to 8 h at 127 °C gave a relatively clear solution, which, on addition of W_{12}, produced crystals of **1**. Apparently, the formation of W_2Al_{28} is not achieved by just mixing the ions but requires the δ-Al_{13} precursors to dimerize. There has been no aluminum heteropolycation species except $GaAl_{12}$ reported so far, and W_2Al_{28} is the first example of an aluminum heteropolycation with transition metal substitution.

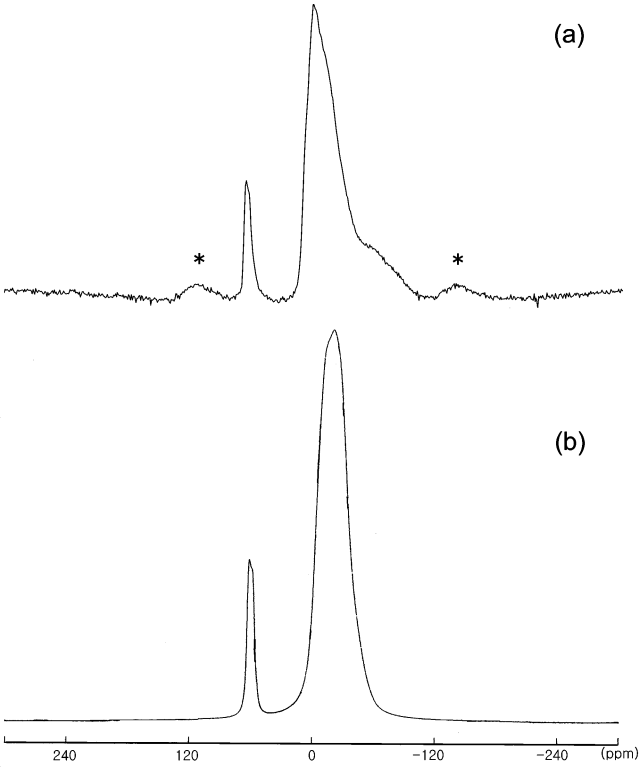

Figure 8. (a) Solid-state ^{27}Al NMR spectrum of **1**. (b) A simulated ^{27}Al NMR spectrum. Spinning sidebands are marked by *.

^{27}Al NMR Spectroscopy of 1 and 2. Figure 8 shows the solid-state ^{27}Al NMR spectrum of **1**. Compound **2** gives essentially the identical spectrum. The sharp peak at 64.7 ppm can be assigned to the tetrahedral Al in the center of δ-Al_{13}, and the peak near 0 ppm is from the octahedral Al in δ-Al_{13} in the periphery. The peak area integration ratio of the tetrahedral Al and the octahedral Al is 1:11.4, which is close to the theoretical value of 1:12. The simulated ^{27}Al NMR spectrum in Figure 8 using the quadrupole parameters estimated from the single-crystal data and a point charge model matches reasonably well with the experimental data. From in situ NMR studies of a ϵ-Al_{13} solution under a forced hydrolysis condition at 127 °C, Taulelle et al. have observed a transient species with δ = 64.5 ppm that occurs during the conversion of ϵ-Al_{13} into Al_{30}.[6] Nazar and co-workers, who have reported the crystal structure of a sulfate salt of δ-Al_{13}, suggested that δ-Al_{13} is the intermediate and is

(26) Adams, D. M. *Inorganic Solids. An Introduction to Concepts in Solid-state Structural Chemistry*; John Wiley & Sons: London, 1974; Chapter 3.

responsible for the $\delta = 64.5$ ppm peak.[7,27] However, the very small amount of their crystals precluded ^{27}Al NMR experiments to verify their suggestion. Therefore, with the single-crystal structures and the NMR data, the present work provides direct and conclusive evidence to the elusive identification of the $\delta = 64.5$ ppm species as δ-Al_{13}.

Conclusion

In this study, we have obtained single crystals of $[\delta\text{-}Al_{13}O_4(OH)_{24}(H_2O)_{12}][XW_{12}O_{40}](OH)\cdot nH_2O$ ($X = H_2$ and Co, $n \cong 20$) and $[W_2Al_{28}O_{18}(OH)_{48}(H_2O)_{24}][H_2W_{12}O_{40}]_2\cdot 55H_2O$ by reacting aluminum polycation $[Al_{30}O_8(OH)_{56}(H_2O)_{26}]^{18+}$ with metatungstate ($H_2W_{12}O_{40}^{6-}$) or tungstocobaltate ($Co^{II}W_{12}O_{40}^{6-}$) in aqueous solutions, determined their crystal structures, and characterized the crystals by the solid-state ^{27}Al NMR. The crystal structures show that the polycations and the POMs are packed mainly by face-to-face interactions through hydrogen bonds and electrostatic interactions. The formation of unusual polycations δ-Al_{13} and W_2Al_{28} may have resulted from the fragmentation of Al_{30} and recombination of the resultant δ-Al_{13}. The solid-state ^{27}Al NMR spectra of the crystals **1** and **2** show a characteristic Al_{Td} peak of δ-Al_{13} at 64.7 ppm, which concludes the long-standing speculation on the identity of the intermediate species in the transformation of ϵ-Al_{13} into Al_{30}.

Acknowledgment. We thank Dr. Y. Do and J.-W. Hwang at KAIST and CMDS for the X-ray single crystal data. The work was supported by the CNNC at SKKU.

Supporting Information Available: Detailed crystallographic data for $[\delta\text{-}Al_{13}O_4(OH)_{24}(H_2O)_{12}][H_2W_{12}O_{40}](OH)\cdot 22H_2O$, $[\delta\text{-}Al_{13}O_4(OH)_{24}(H_2O)_{12}][CoW_{12}O_{40}](OH)\cdot 19H_2O$, and $[W_2Al_{28}O_{18}(OH)_{48}(H_2O)_{24}][H_2W_{12}O_{40}]_2\cdot 55H_2O$ in CIF format. This material is available free of charge via the Internet at http://pubs.acs.org.

IC0340377

(27) Fu, G.; Nazar, L. F.; Bain, A. D. *Chem. Mater*. **1991**, *3*, 602.